Synthetic Metals 234 (2017) 95–99

Contents lists available at ScienceDirect

Synthetic Metals

journal homepage: www.elsevier.com/locate/synmet

Research paper

Effects of acceptor on the performance of exciplex-based OLED

Tong Lin[a,b], Qiaogang Song[a,b], Zheqin Liu[a,b], Bei Chu[a], Wenlian Li[a], Yongshi Luo[a], C.S. Lee[c], Zisheng Su[a,*], Yantao Li[a,*]

[a] State Key Laboratory of Luminescence and Applications, Changchun Institute of Optics, Fine Mechanics and Physics, Chinese Academy of Sciences, Changchun 130033, PR China

[b] University of Chinese Academy of Sciences, Beijing 100039, PR China

[c] Center of Super-Diamond and Advanced Films (COSDAF) and Department of Physics and Materials Sciences, City University of Hong Kong, Hong Kong SAR, PR China

ARTICLE INFO

Keywords:
TADF
OLED
Exciplex
PLQY
Charge carrier balance

ABSTRACT

In this work, exciplex-based OLEDs (ExOLEDs) are fabricated with 1,1-bis((di-4-tolylamino)phenyl)cyclohexane (TAPC) as the donor and a series triazine derivatives, e.g., 2,4,6-tris(biphenyl-3-yl)-1,3,5-triazine (T2T), 2,4,6-tris(3-(1H-pyrazol-1-yl)phenyl)-1,3,5-triazine (3P-T2T), and 2,4,6-tris(m-(diphenylphosphinoyl)phenyl)-1,3,5-triazine (PO-T2T), as the acceptors. With different acceptors and mole ratios of donor:acceptor, the effects of the photoluminescence quantum yield (PLQY), charge carrier balance, and exciton lifetime on the EQE and efficiency roll-off are systematically investigated. It is found that the external quantum efficiency (EQE) of the ExOLEDs is primary determined by the PLQY of the mixed donor:acceptor film and tuned in a certain extent by the charge carrier balance. Furthermore, the efficiency roll-offs of different ExOLEDs are all less than 20%, which are simultaneously determined by the photoluminescence (PL) lifetime and the charge carrier balance.

1. Introduction

Thermally activated delayed fluorescence (TADF) organic light-emitting diodes (OLEDs) have attracted great attention in the past few years for their applications in next generation display and lighting [1–12]. TADF is a promising mechanism to use non-radiative triplet excitons for light emission by efficient reverse intersystem crossing (RISC) via thermal activation. Thus, OLEDs based on TADF emitters can attain 100% internal quantum efficiency in theory, which are the same as phosphorescent OLEDs [13,14]. To achieve efficient RISC, a small energy difference between the singlet and the triplet excited states ($\triangle E_{ST}$) is required. Organic intramolecular TADF materials are composed of electron donor and acceptor groups in a molecule to attain efficient TADF, which are hard to design. In addition to intramolecular TADF materials, small $\triangle E_{ST}$ can be realized by exciplex formation via intermolecular charge transfer between donor and acceptor molecules [15–19]. However, there are few exciplex-based OLEDs (ExOLEDs) reported with high external quantum efficiencies (EQEs) [20–28]. Besides, the efficiency roll-off is another figure-of-merit factor for an ExOLED. To attain a high EQE with a low efficiency roll-off, it is necessary to understand which factors that limited these parameters of an ExOLED.

2. Methods

The photoluminescence quantum yield (PLQY) was measured with F900 fluorescence spectrometer (Edinburgh Instruments Ltd) and the system combined with an integrating sphere, a Xe lamp (as the excitation source) and a multichannel spectrometer (as the optical detector). The mobilities were measured by steady-state space-charge limited currents (SCLC) method. The structures of hole and electron only devices were ITO/MoO_3 (20 nm)/test layer (100 nm)/MoO_3 (20 nm)/Al (100 nm) and ITO/C_{60} (20 nm)/test layer (100 nm)/C_{60} (20 nm)/Al (100 nm), respectively. ITO coated glasses were pre-cleaned and treated with ultraviolet-ozone for 15 min before fabrication of OLEDs. All layers were thermally evaporated in a vacuum chamber under about 4×10^{-4} Pa. All organic materials were purchased without further purification. Absorption spectra were measured on a Shimadzu UV-3101PC spectrophotometer. Steady-state photoluminescence (PL) and electroluminescence (EL) spectra were obtained from a Shimadzu F7000 and OPT-2000 spectrophotometers, respectively. Transient PL decay was measured with FL920 (Edinburgh Instruments Ltd). The electrical properties of devices and mobility of blended layers were measured with a Keithley 2400 source meter under ambient condition. EQE was calculated from the current density, luminance, and EL spectrum, assuming a Lambertian distribution.

* Corresponding authors.
E-mail addresses: suzs@ciomp.ac.cn (Z. Su), liyt@ciomp.ac.cn (Y. Li).

http://dx.doi.org/10.1016/j.synthmet.2017.10.013
Received 25 August 2017; Received in revised form 18 October 2017; Accepted 19 October 2017
Available online 05 November 2017
0379-6779/ © 2017 Elsevier B.V. All rights reserved.

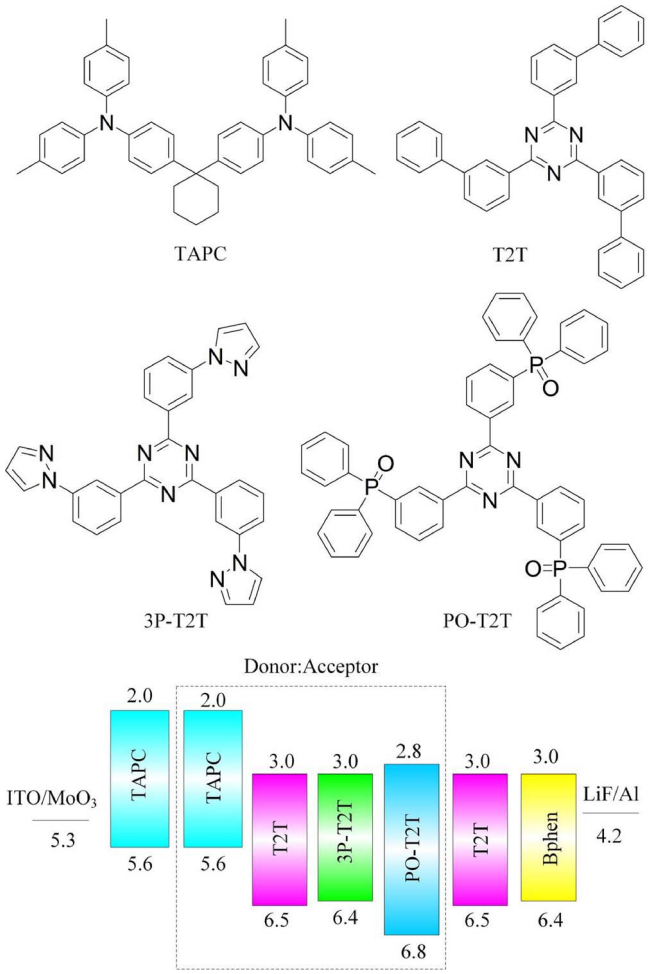

Fig. 1. Molecular structures of the materials and the schematic energy level diagram of the device.

3. Results and discussion

In our previous study, we reported an ExOLED by using 1,1-bis((di-4-tolylamino)phenyl)cyclohexane (TAPC) and 2,4,6-tris(biphenyl-3-yl)-1,3,5-triazine (T2T) as the donor and acceptor, respectively [26]. This ExOLED shows an EQE of 11.6%, which is one of the highest among the reported ones [22–26]. In this study, ExOLEDs are fabricated with TAPC as the donor material and T2T, 2,4,6-tris(3-(1H-pyrazol-1-yl) phenyl)-1,3,5-triazine (3P-T2T), and 2,4,6-tris(m-(diphenylphosphinoyl)phenyl)-1,3,5-triazine (PO-T2T) as the acceptor materials, respectively. These three acceptor materials are selected because they have similar molecular structures with a triazine core in the molecules (Fig. 1) but different energy levels and electron mobilities. The structure of the ExOLEDs is ITO/MoO_3 (3 nm)/TAPC (25 nm)/TAPC:acceptor (15 nm)/T2T (5 nm)/Bphen (30 nm)/LiF (1 nm)/Al (100 nm). A schematic energy level diagram of the device is also shown in Fig. 1 with the energy level data cited from references [19,29–32]. Combining with the photoluminescence and charge carrier transporting properties, we systematically investigated the factors that limiting the EQE and efficiency roll-off of the ExOLEDs.

The current density-voltage-luminance characteristics of the ExOLEDs with different donor and acceptor mixing mole ratios are shown in Fig. S1. It can be found that these characteristics are significantly affected by the mixing ration. Fig. 2 presents the EQEs of the ExOLEDs, and the maximum EQEs derived from these curves are listed in Table 1. Among the three series devices, the devices based on TAPC:T2T show the highest EQE. The maximum EQEs are 11.6%, 6.5%, and 5.1%, respectively, for the TAPC:T2T, TAPC:3P-T2T, and TAPC:PO-T2T based devices.

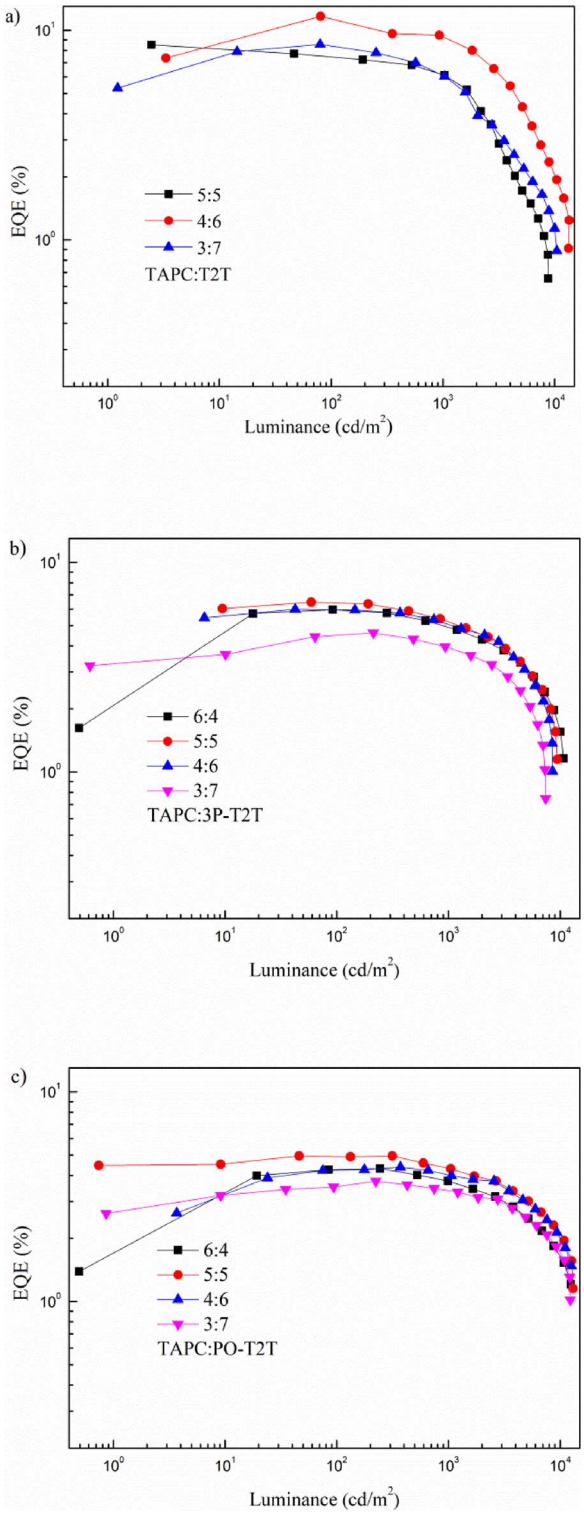

Fig. 2. EQE-luminance characteristics of (a) TAPC:T2T, (b) TAPC:3P-T2T, and (c) TAPC:PO-T2T based devices with different mixing ratios.

The theoretical EQE of an OLED can be calculated from equation:

$$EQE = \gamma \eta_r \eta_{PL} \eta_{OUT} \quad (1)$$

where γ is the ratio of the charge combination to the electron and hole transportation, η_r is the ratio of exciton formation for radiative transition, η_{PL} is the photoluminescence quantum yield (PLQY), and η_{out} is

Table 1
The performance of different EMLs.

EMLs	Mix ratio	EQE (%)	PLQY (%)	μ_h (cm^2/V s)	μ_e (cm^2/V s)
TAPC:T2T	5:5	8.6	75	5.0×10^{-4}	1.1×10^{-6}
	4:6	11.6	69	1.2×10^{-4}	3.0×10^{-6}
	3:7	8.5	64	6.1×10^{-5}	7.7×10^{-6}
TAPC:3P-T2T	6:4	6.0	34	5.6×10^{-4}	8.9×10^{-6}
	5:5	6.5	31	4.4×10^{-4}	1.3×10^{-5}
	4:6	6.0	28	1.1×10^{-4}	5.2×10^{-5}
	3:7	4.7	27	4.5×10^{-5}	9.1×10^{-5}
TAPC:PO-T2T	6:4	4.3	28	5.7×10^{-4}	8.6×10^{-6}
	5:5	5.1	25	3.3×10^{-4}	1.0×10^{-5}
	4:6	4.4	21	1.6×10^{-4}	4.8×10^{-5}
	3:7	3.7	19	4.3×10^{-5}	1.1×10^{-4}

the out-coupling constant [11]. η_r of an ExOLED is assumed to be unity, because both the singlet and triplet excited states can contribute to the emission. η_{out} is determined by the device configuration and the refractive indexes of the materials used. Except for microcavity effect and so on [33,34], η_{out} is about 20%-30% for a traditional OLED. Thus, the EQE is usually determined by the other two factors. However, it still uncertain which is the primary one.

First, we investigate the PL properties of the devices. Fig. 3 shows the PL spectra of pristine TAPC, T2T, 3P-T2T, and PO-T2T films and the mixed TAPC:T2T, TAPC:3P-T2T, and TAPC:PO-T2T films. The PL wavelength peaks of pristine TAPC, T2T, 3P-T2T, and PO-T2T films are located at about 384, 399, 410, and 397 nm, respectively. The emissions of the three acceptors display a blue-shift from T2T to 3P-T2T and PO-T2T, which is consistent with the bandgaps of these materials. On contrast, the PL emissions are located at about 517, 555, and 563 nm for TAPC:T2T, TAPC:3P-T2T, and TAPC:PO-T2T films, respectively. These emissions are dramatically red-shifted compared to their respective donor and acceptor. The EL spectra of TAPC:T2T, TAPC:3P-T2T and TAPC:PO-T2T based devices are not affected by the mixing ratio of the donor and acceptor, and their peak wavelengths are 528, 568, and 577 nm, respectively, as shown in Fig. 4. It can be found that the EL spectra are red-shifted about 10 nm compared to their respective PL spectra. Due to the higher hole mobility of TAPC than the electron mobility of the acceptors (which will be characterized latter), the hole and electron recombination zone will locate at the emitting layer/T2T interface at lower voltage and shift to the anode side at higher voltage. Thus both the bulk exciplex formed between the donor and acceptor and the interface exciplex formed between the donor and the electron transporting layer T2T are expected. However, the EL spectra of devices almost have no change with the voltages, as shown in Fig. S2. This means that the recombination is primary in the emitting layers and there is no energy transfer between the bulk exciplex and interface

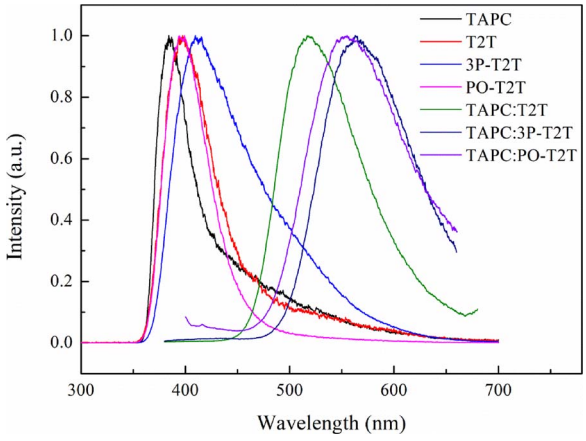

Fig. 3. PL spectra of TAPC, T2T, 3P-T2T, PO-T2T, TAPC:T2T, TAPC: 3P-T2T, and TAPC:PO-T2T films.

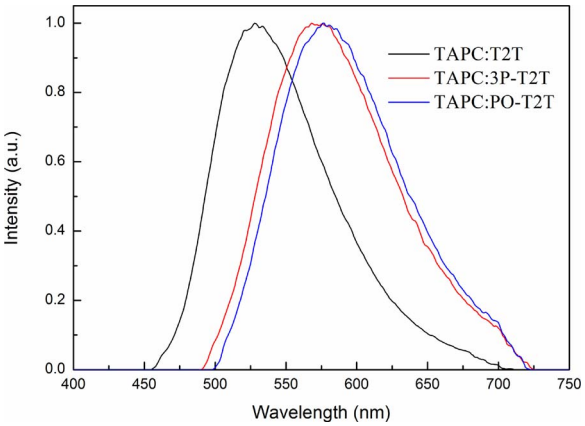

Fig. 4. EL spectra of TAPC:T2T, TAPC: 3P-T2T, and TAPC:PO-T2T devices at 5 V.

exciplex [28,35,36].

We have measured the transition PL decay curves of the exciplexes monitored at their respective PL peaks with a 310 nm excitation at 300 K, and found that the curves are almost consistent with different donor:acceptor mixing ratio. Fig. 5 shows the typical transition PL decay curves of the three exciplexes. The decays can be fitted by the formula as follows:

$$I(t) = A_1 \exp(-t/\tau_1) + A_2 \exp(-t/\tau_2) \quad (2)$$

All the three decay curves have a prompt component and a delayed component, showing the TADF character of these exciplexes. The calculated lifetimes of the prompt and delayed components are listed in Table 2. The lifetimes of the prompt components range from 19 to 32 ns while those from 1.1 to 2.9 μs for the delayed components.

Table 1 listed the PLQYs of the three series donor:acceptor films with different mixing mole ratios. Under 310 nm excitation, the PLQYs of TAPC:T2T films range from 64% to 75%, while they are from 27% to 34% for TAPC:3P-T2T and 19% to 28% for TAPC:PO-T2T. Among these three series films, the TAPC:T2T films exhibit the highest PLQY, which is consistent with the EQE of the devices. This indicates that a higher PLQY always leads to a higher EQE, and similar results have been reported in other papers [21,22,24]. It should be noted that in each series devices, the highest EQE is not obtained from the ones with the highest PLQY. For example, the TAPC:T2T film with the mixing ratio of 5:5 exhibits a PLQY of 75%, while the corresponding device shows an EQE of only 8.6%. However, the TAPC:T2T film with mixing ratio of 4:6 exhibits a PLQY of 69%, while the corresponding device shows a highest EQE of 11.6%. This suggests that there are other factors that limiting the EQE of the devices.

On the other hand, the PLQY of the films decreases with the

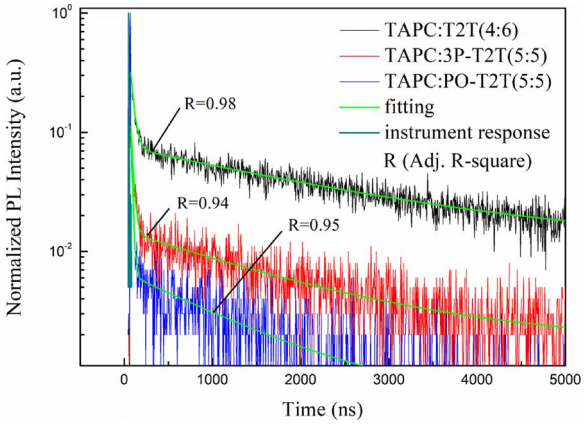

Fig. 5. PL decay curves of TAPC:T2T, TAPC: 3P-T2T, and TAPC:PO-T2T films at 300 K.

Table 2
Parameters of different exciplexes.

Film	τ_1(ns)	τ_2(ns)	$\triangle E_{ST}$	IQE	Roll-off [a]
TAPC:T2T(4:6)	31.6	2897	21	0.68	19%
TAPC:3P-T2T(5:5)	32	1598	26	0.29	17%
TAPC:PO-T2T(5:5)	19.8	1139	57	0.20	13%

[a] decrease of EQE from maximum to 1000 cdm^{-2}.

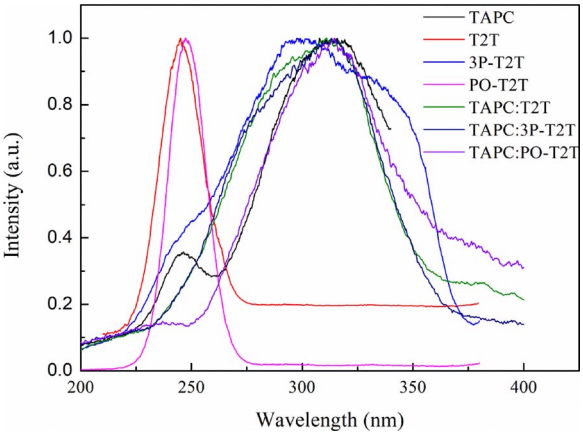

Fig. 6. Excitation spectra of TAPC, T2T, 3P-T2T, PO-T2T,TAPC:T2T, TAPC:3P-T2T, and TAPC:PO-T2T films.

decrease of the mixing ratio of TAPC component, as shown in Table 1. This phenomenon has also been observed in our previous work [37]. Under optical excitation, the exciplex is formed through charge transfer from one excited donor (acceptor) molecule to one ground acceptor (donor) molecule with the formula of:

$$D + A \xrightarrow{h\nu} D^* + A(orD + A^*) \rightarrow D^+A^- \quad (3)$$

where D and A represent donor and acceptor, respectively, and D^+A^- is the charge transfer state (exciplex). Under such a formula, the optimized mole ratio of the donor and acceptor should be 1:1. This is contrary to the findings in PLQY. To further understand the mechanisms, the excitation spectra of the films are investigated in Fig. 6. The excitation peak of TAPC locates at about 310 nm, while they are 245, 286, and 248 nm for T2T, 3P-T2T, and PO-T2T, respectively. Interestingly, the excitation peaks of the TAPC:T2T, TAPC:3P-T2T, and TAPC:PO-T2T are all located at about 310 nm, indicating that most of the exciplex emission comes from the excitation of TAPC in the mixed films. This suggests the donor TAPC is easier to be excited to its excited state and/or the charge transfer efficiency is higher from TAPC to the acceptors than from the acceptors to TAPC. Therefore, the PLQY of the mixed films increases with the content of TAPC.

The PLQY of the mixed films based on TADF of exciplexes is highly determined by $\triangle E_{ST}$, and a smaller $\triangle E_{ST}$ will result in a higher PLQY. The $\triangle E_{ST}$ can be expressed with the equation [22]:

$$\Delta E_{ST} = RT\ln(K_{eq}/3) \quad (4)$$

where R is the ideal gas constant, T is the absolute temperature, K_{eq} is the equilibrium constant, and the factor of 3 stands for the triplet degenerate states. K_{eq} can be obtained by the ratio of A_1 and A_2 in Eq. (2). The $\triangle E_{ST}$ of the TAPC:T2T, TAPC:3P-T2T, and TAPC:PO-T2T films are calculated to be 21, 26, and 57 meV, respectively, as listed in Table 2. These values are consistent with the PLQY of the mixed films. These findings suggest that if the donor:acceptor system has a low $\triangle E_{ST}$, it will show a high PLQY and a high EQE of the device.

The exciplex emission energy ($h\nu_{exciplex}$) can be described as [38]:

$$h\nu_{exciplex} = I_D - A_A - E_C \quad (5)$$

where I_D is the ionization energy of the donor, A_A is the electronic affinity of the acceptor, E_C is the Coulomb interaction between the excess electron on the acceptor and the excess hole in the donor. From the energy levels of the materials and the PL emissions of the films shown in Figs. 1 and 3, the E_C of TAPC:T2T, TAPC:3P-T2T, and TAPC:PO-T2T are calculated to be 0.2, 0.4, and 0.6 eV, respectively. The small Ec may indicate a large space distance between the electron donor and acceptor molecules, which leads to a small $\triangle E_{ST}$ [15,16]. According to this rule, TAPC:T2T will be assumed to have a lowest $\triangle E_{ST}$, which is consistent with the values calculated from Eq. (4).

Another factor determining the EQE of the devices is γ, which reflects the charge carrier balance of the devices. To evaluate the charge carrier balance, we use a simple method of steady-state space-charge limited currents (SCLC) to determine the charge carrier mobility of the mixed films. Without considering diffusion, SCLC in a trap-free insulator is given by the Mott–Gurney equation:

$$j_{SCLC} = \frac{9}{8}\varepsilon_0\varepsilon_r\mu\frac{(V - V_{bi})^2}{d^3} \quad (6)$$

where ε_0 is the absolute permittivity of the free space, ε_r is the relative dielectric constant of the material, d is the thickness of devices, and V-V_{bi} is the applied voltage minus the built-in voltage. Mobility values from SCLC can be considered as a lower estimation for the mobility [39]. The electric field dependencies of hole and electron drift mobilities for the layers of different exciplexes are shown in Fig.S3. With the method of SCLC, the hole mobility of TAPC is estimated to be 1.6×10^{-3} $cm^2V^{-1}s^{-1}$, while the electron mobility of T2T, 3P-T2T, and PO-T2T are 2.7×10^{-5}, 1.1×10^{-4}, and 2.2×10^{-4} $cm^2V^{-1}s^{-1}$ at 6×10^5 Vcm^{-1}, respectively. It can be found that the hole mobility of TAPC is at least one order of magnitude higher than the electron mobility of the three acceptors.

The SCLC method has been used to investigate the hole and electron mobilities of the mixed active layer of an organic solar cell [40]. In the same way, it is applied to our donor:acceptor mixed emitting layers, and pertinent data are summarized in Table 1. It can be found that the hole mobility of the mixed films decreases with the decreased content of the donor, and a similar trend is found for electron mobility. Besides, the hole mobility of the three series mixed films is higher than their respective electron mobility in the mixed ratio used here. This can be reasonably understood due to the higher hole mobility of TAPC than the electron mobility of the three acceptors as found above. Among the three series mixed films, the TAPC:PO-T2T series has the highest electron mobility. From the energy level diagram shown in Fig. 1, there is no energy barrier for holes inject to the emitting layer due to TAPC is used as both the hole transporting layer and donor material, while there is a 0.2 eV barrier for electron injection from T2T to PO-T2T. The highest electron mobility of the TAPC:PO-T2T films suggests that this a small barrier has a little effect on the electron injection efficiency and hence the EQE of the devices. Although the TAPC:T2T series has the lowest electron mobility of in the order of 10^{-6} $cm^2V^{-1}s^{-1}$, which indicates that the ratio between the hole and electron mobilities in the ExOLEDs can reach up to two orders of magnitude, this series devices have the highest EQE among the three series. This should be attributed to the higher PLQY of the TAPC:T2T films, which is more than twice to that of TAPC:3P-T2T and TAPC:PO-T2T films. On the other hand, the highest EQE is not found in the devices with neither the highest PLQY nor the highest charge carrier balance. For example, in the TAPC:T2T based devices, the highest EQE is found with a TAPC:T2T mixed ratio of 4:6, which has the moderate PLQY and charge carrier balance among the three devices.

Under electrical excitation, the internal quantum efficiency (IQE) of TADF OLEDs could be calculated with the formula:

$$IQE = \eta_r(S_1)\Phi_{PF} + [\eta_r(T_1) + \eta_r(S_1)(1 - \Phi_{PF})]\frac{\Phi_{DF}}{(1 - \Phi_{PF})} \quad (7)$$

where $\eta_r(S_1)$ and $\eta_r(T_1)$ are the branching ratio of singlet and triplet

exciton formations, respectively. Φ_{PF} and Φ_{DF} are prompt and delayed components of PLQY, which are calculated by Eqution S1. Thus, IQEs of TAPC:T2T, TAPC:3P-T2T, and TAPC:PO-T2T are calculated to be 0.68, 0.29, and 0.20, respectively, as listed in Table 2. Assuming a light out-coupling efficiency is 20–30% and γ and η_r are 1, the EQE of the three devices are in the range of 13.6 to 20.4%, and 5.8 to 8.7%, and 4.0 to 6.0%, respectively. It can be found that the calculated EQE of TAPC:T2T device has a largest deviation from that measured. In this calculation, the charge carrier balance factor is not considered. In account of the largest difference between the hole- and electron-mobilities in T-APC:T2T device, this largest deviation can be reasonably understood. This suggests that charge balance indeed plays a role in determining the EQE of the devices.

Based on the discussion above, it can be found that the EQE of an ExOLED is primary determined by the PLQY of the mixed donor:-acceptor film, and the charge carrier balance can also tune the EQE in a certain extent. Under photoexcitation, the exciplexes are formed primary through the excitation of the donor TAPC. Thus, the mixed films will show a higher PLQY with a higher content of TAPC. However, the hole mobility of TAPC is about two orders of magnitude higher than the acceptors. Increasing the TAPC content will result in a further unbalance of the charge carrier injection. In such a situation, a higher EQE could be expected if a suitable acceptor with a higher electron mobility were used. However, this is challenging and there is rare electron transporting materials showing a comparable electron mobility to the hole mobility of most hole transporting materials. This problem could be resolved if the exciplex were formed primary through the excitation of the acceptor material. Then the PLQY and charge carrier balance can be simultaneously improved by increasing the ratio of the acceptor component.

In addition to EQE, efficiency roll-off is another figure-of-merit parameter of an OLED. The efficiency roll-off of the TAPC:T2T, TAPC:3P-T2T, and TAPC:PO-T2T devices are 19%, 17%, and 13%, respectively, as listed in Table 2. Although TAPC:PO-T2T device presents the lowest EQE, it exhibits a smallest efficiency roll-off. The efficiency roll-off of a ExOLED is resulted from triplet exciton quenching, such as single-triplet exciton annihilation [41], triplet–triplet exciton annihilation [42], and triplet-polaron annihilation [43]. This indicates that the device with a short exciton lifetime and a balanced hole and electron mobility will show a smallest efficiency roll-off. This is consistent with the PL lifetime and charge balance character of the three devices.

4. Conclusion

In summary, ExOLEDs with TAPC as the donor and T2T, 3P-T2T, or PO-T2T as the acceptor are constructed and the factors that determining the EQE and efficiency roll-off of the devices are systematically investigated. It has been found that the EQE of the ExOLEDs is primary determined by the PLQY of the mixed donor:acceptor film and tuned in a certain extent by the charge carrier balance. On the other hands, the efficiency roll-off of the ExOLEDs is simultaneously determined by the PL lifetime and the charge carrier balance. Thus, a high efficiency and low efficiency roll-off ExOLED can be expected if the device has a high PLQY, a short exciton lifetime, and a balanced charge carrier mobility. This work provides some criterions on selecting materials and designing the structure of ExOLED, which may have the potential application to develop high performance ExOLEDs.

Acknowledgements

This work was supported by the National Natural Science Foundation of China (61575192, 61376022, and 61376062).

Appendix A. Supplementary data

Supplementary data associated with this article can be found, in the online version, at https://doi.org/10.1016/j.synthmet.2017.10.013.

References

[1] H. Uoyama, K. Goushi, K. Shizu, H. Nomura, C. Adachi, Nature 492 (2012) 234.
[2] G. Mehes, H. Nomura, Q.S. Zhang, T. Nakagawa, C. Adachi, Angew. Chem. Int. Edit. 51 (2012) 11311.
[3] S.Y. Lee, T. Yasuda, H. Nomura, C. Adachi, Appl. Phys. Lett. 101 (2012) 093306.
[4] H. Tanaka, K. Shizu, H. Miyazaki, C. Adachi, Chem. Commun. 48 (2012) 11392.
[5] T. Nakagawa, S.Y. Ku, K.T. Wong, C. Adachi, Chem. Commun. 48 (2012) 9580.
[6] Q.S. Zhang, J. Li, K. Shizu, S.P. Huang, S. Hirata, H. Miyazaki, C. Adachi, J. Am. Chem. Soc. 134 (2012) 14706.
[7] J. Li, T. Nakagawa, J. MacDonald, Q.S. Zhang, H. Nomura, H. Miyazaki, C. Adachi, Adv. Mater. 25 (2013) 3319.
[8] F.B. Dias, K.N. Bourdakos, V. Jankus, K.C. Moss, K.T. Kamtekar, V. Bhalla, J. Santos, M.R. Bryce, A.P. Monkman, Adv. Mater. 25 (2013) 3707.
[9] Q.S. Zhang, B. Li, S.P. Huang, H. Nomura, H. Tanaka, C. Adachi, Nat. Photon. 8 (2014) 326.
[10] H. Wang, L.S. Xie, Q. Peng, L.Q. Meng, Y. Wang, Y.P. Yi, P.F. Wang, Adv. Mater. 26 (2014) 5198.
[11] Y. Tao, K. Yuan, T. Chen, P. Xu, H.H. Li, R.F. Chen, C. Zheng, L. Zhang, W. Huang, Adv. Mater. 26 (2014) 7931.
[12] D.D. Zhang, L. Duan, Y.G. Zhang, M.H. Cai, D.Q. Zhang, Y. Qiu, Light-Sci. Appl. 4 (2015) e232.
[13] M.A. Baldo, S. Lamansky, P.E. Burrows, M.E. Thompson, S.R. Forrest, Appl. Phys. Lett. 75 (1999) 4.
[14] X. Li, H.J. Chi, G.H. Lu, G.Y. Xiao, Y. Dong, D.Y. Zhang, Z.Q. Zhang, Z.Z. Hu, Org. Electron. 13 (2012) 3138.
[15] K. Goushi, K. Yoshida, K. Sato, C. Adachi, Nat. Photon. 6 (2012) 253.
[16] K. Goushi, C. Adachi, Appl. Phys. Lett. 101 (2012) 023306.
[17] V. Jankus, C.J. Chiang, F. Dias, A.P. Monkman, Adv. Mater. 25 (2013) 1455.
[18] S. Lee, K.H. Kim, D. Limbach, Y.S. Park, J.J. Kim, Adv. Funct. Mater. 23 (2013) 4105.
[19] W.-Y. Hung, G.-C. Fang, Y.-C. Chang, T.-Y. Kuo, P.-T. Chou, S.-W. Lin, K.-T. Wong, ACS Appl. Mater. Interfaces 5 (2013) 6826.
[20] L. Zhang, C. Cai, K.F. Li, H.L. Tam, K.L. Chan, K.W. Cheah, ACS Appl. Mater. Interfaces 7 (2015) 24983.
[21] J. Li, H. Nomura, H. Miyazaki, C. Adachi, Chem. Commun. 50 (2014) 6174.
[22] W.Y. Hung, P.Y. Chiang, S.W. Lin, W.C. Tang, Y.T. Chen, S.H. Liu, P.T. Chou, Y.T. Hung, K.T. Wong, Acs Appl. Mater. Interfaces 8 (2016) 4811.
[23] W. Liu, J.X. Chen, C.J. Zheng, K. Wang, D.Y. Chen, F. Li, Y.P. Dong, C.S. Lee, X.M. Ou, X.H. Zhang, Adv. Funct. Mater 26 (2016) 2002.
[24] X.K. Liu, Z. Chen, C.J. Zheng, C.L. Liu, C.S. Lee, F. Li, X.M. Ou, X.H. Zhang, Adv. Mater. 27 (2015) 2378.
[25] Y.S. Park, K.H. Kim, J.J. Kim, Appl. Phys. Lett 102 (2013) 153306.
[26] T. Lin, T. Zhang, Q. Song, F. Jin, Z. Liu, Z. Su, Y. Luo, B. Chu, C.S. Lee, W. Li, Org. Electron 38 (2016) 69.
[27] K.H. Kim, S.J. Yoo, J.J. Kim, Chem. Mater. 28 (2016) 1936.
[28] E. Skuodis, A. Tomkeviciene, R. Reghu, L. Peciulyte, K. Ivaniuk, D. Volyniuk, O. Bezvikonnyi, G. Bagdziunas, D. Gudeika, J.V. Grazulevicius, Dyes Pigm. 139 (2017) 795–807.
[29] H. Sasabe, Y. Seino, M. Kimura, J. Kido, Chem. Mater. 24 (2012) 1404.
[30] H.W. Mo, Y. Tsuchiya, Y. Geng, T. Sagawa, C. Kikuchi, H. Nakanotani, F. Ito, C. Adachi, Adv. Funct. Mater. 36 (2016) 6703.
[31] T. Zhang, B. Zhao, B. Chu, W. Li, Z. Su, X. Yan, C. Liu, H. Wu, Y. Gao, F. Jin, F. Hou, Sci. Rep. 5 (2015) 10234.
[32] W.Y. Hung, G.C. Fang, S.W. Lin, S.H. Cheng, K.T. Wong, T.Y. Kuo, P.T. Chou, Sci. Rep. 4 (2014) 5161.
[33] C.Y. Xiang, W. Koo, F. So, H. Sasabe, J. Kido, Light-Sci. Appl. 2 (2013) e72.
[34] J. Lee, M. Slootsky, K. Lee, Y.F. Zhang, S.R. Forrest, Light-Sci. Appl. 3 (2014) e181.
[35] M. Cekaviciute, J. Simokaitiene, D. Volyniuk, G. Sini, J.V. Grazulevicius, Dyes Pigm. 140 (2017) 187–202.
[36] R. Butkute, R. Lygaitis, V. Mimaite, D. Gudeika, D. Volyniuk, G. Sini, J.V. Grazulevicius, Dyes Pigm. 146 (2017) 425–437.
[37] T. Zhang, B. Chu, W. Li, Z. Su, Q.M. Peng, B. Zhao, Y. Luo, F. Jin, X. Yan, Y. Gao, ACS Appl. Mater. Interfaces 6 (2014) 11907.
[38] M. Mazzeo, D. Pisignano, F. Della Sala, J. Thompson, R.I.R. Blyth, G. Gigli, R. Cingolani, G. Sotgiu, G. Barbarella, Appl. Phys. Lett. 82 (2003) 334–336.
[39] O.J. Weiss, R.K. Krause, A. Hunze, J. Appl. Phys. 103 (2008) 043709.
[40] C.T. Lee, C.H. Lee, Org. Electron 14 (2013) 2046–2050.
[41] N.C. Giebink, S.R. Forrest, Phys. Rev. B 77 (2008) 235215.
[42] M.A. Baldo, C. Adachi, S.R. Forrest, Phys. Rev. B 62 (2000) 10967.
[43] S. Reineke, K. Walzer, K. Leo, Phys. Rev. B 75 (2007) 125328.